EPJ Web of Conferences **380**, 02006 (2026) https://doi.org/10.1051/epjconf/202638002006
ICISCT'25

Techno-Economic Energy Management of an AC Multi-Microgrid

Ayoub Chrif[1,2,3*], Elhoussin Elbouchikhi[4], Abdelmajid Abouloifa[2], and Mohamed Machmoum[1]

[1]IREENA, Nantes University, Saint-Nazaire, France
[2]ESE Laboratory, ENSEM, Hassan II University, Casablanca, Morocco
[3]LABISEN, ISEN Yncrea Ouest, Nantes, France
[4]SATIE UMR CNRS 8029, CY Cergy-Paris University, Cergy, France

Abstract. This study presents a comprehensive techno-economic optimization framework for AC multi-microgrid (MMG) systems. A dynamic energy management system (EMS) is developed to coordinate the operation of distributed energy resources (DERs), minimize total operational costs, and reduce dependency on the main grid. The EMS efficiently manages energy exchanges between microgrids, optimizes battery charging and discharging strategies, and ensures a balanced integration of renewable energy sources. Simulation results for a case study in Casablanca, Morocco, validate the effectiveness of the proposed approach, demonstrating cost reductions, improved renewable energy utilization, and decreased reliance on the external grid through coordinated real-time energy management.

1 Introduction

The global energy demand has been increasing steadily due to population growth and socioeconomic advancements. This surge in energy consumption spans across various sectors, underscoring the critical role electricity plays in modern life. To address this, microgrids (MG) provide an effective and adaptable solution. Microgrids are self-contained low to medium-voltage power distribution systems that offer local and decentralized energy supply [1]. They can function in either a grid-connected or standalone mode [2]. Additionally, incorporating renewable energy sources (RES) like solar photovoltaics (PV) and wind turbines (WT) into these systems is becoming more economical, thanks in major part to government interventions such as subsidies and feed-in tariffs [3]. At the same time, energy storage systems (ESS) are emerging as essential components to support the integration of these variable resources, by storing surplus energy during high generation periods and delivering it during times of low production or increased demand.

A multi-microgrid (MMG) is a more advanced form of microgrid, comprising a network of nearby microgrids interconnected physically and digitally. This structure increases operational flexibility, system resilience, and energy performance, optimizing energy management

*Corresponding author: ayoub.chrif@etu.univ-nantes.fr

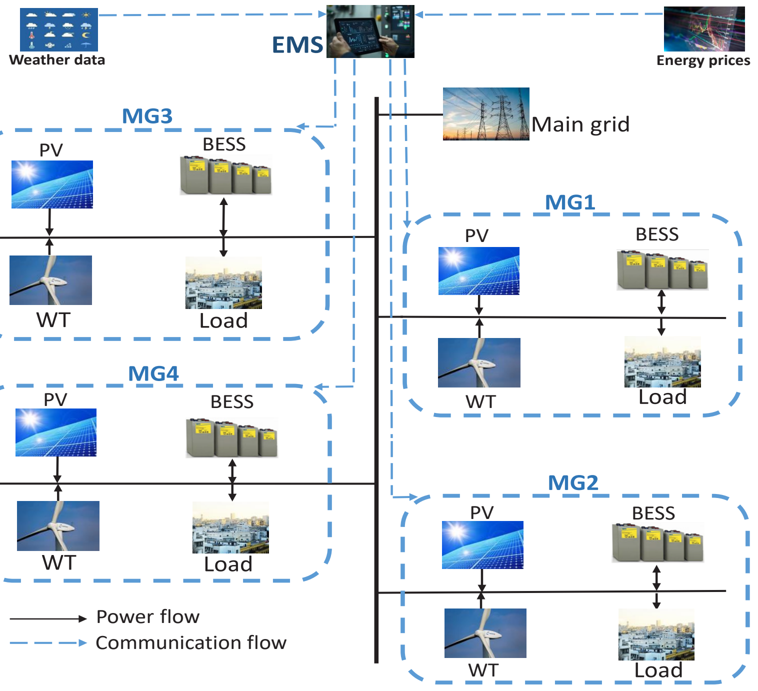

Figure 1. System architecture.

and coordination with both the main grid and among microgrids themselves. The close proximity of these microgrids results in varied electricity consumption patterns, offering chances for renewable energy exchange, thus allowing a more effective and efficient use of renewable resources.

In MMG systems, energy management is crucial for balancing the fluctuating output of RES, the varying load demands, and the dynamic state of charge (SOC) of ESS. Achieving this balance ensures the reliability and stability of the network, optimizes the utilization of local energy resources, and minimizes operational costs. It requires sophisticated control strategies capable of forecasting generation and consumption patterns, coordinating power exchanges between microgrids, and maintaining the optimal performance and lifespan of storage units.

A generalized five-bus microgrid structure is adopted in this study (Fig. 1). The system consists of four geographically distributed microgrids interconnected through distribution lines and connected to the main grid. Each microgrid integrates various distributed energy resources (DER), including PV, WT, and battery ESS (BESS), to satisfy local energy demands. This system is supervised and managed by an energy management system (EMS), which optimizes the MMG's operation and manages power flows [4].

2 MMG Modeling

2.1 PV panels

The PV available power of each MG x at time t is determined by its rated capacity and the prevailing weather conditions, namely the solar irradiance G_t and the ambient temperature

$T_{a,t}$, as expressed by the following relation:

$$P_{pv_{x,t}} = \eta_{pv_x}.A_{pv_x}.G_t.\left(1 - \beta.(T_{a_t} + \frac{NOCT - 20}{G_{NOCT}} \cdot G_t - T_{ref})\right) \tag{1}$$

where, η_{pv} represents the efficiency associated with the PV technology and power conditioning, while A_{pv_x} denotes the panels surface area (in m^2). The parameter β is a temperature coefficient (typically 0.004/°C), T_{ref} is the reference temperature, and G_{NOCT} stands for the irradiance under nominal operating cell temperature (NOCT) conditions.

2.2 Wind turbine

The WT available power in each MG x is calculated using wind speed data and it is expressed as follows:

$$P_{wt_{x,t}} = \frac{1}{2}.C_p.\eta_{wt}.\rho.\pi.R_{wt_x}^2.V_t^3 \tag{2}$$

where V_t is the wind velocity at time t (m/s), ρ denotes the air density (typically 1.225 kg/m^3), R_{wt_x} represents WT radius (in meters), C_p is the performance coefficient of the turbine (commonly around 0.4), and η_{wt} corresponds to WT efficiency.

2.3 Batteries

The battery is characterized by its state of charge (SOC), which evolves over time according to the charging and discharging processes:

$$SOC_{x,t}^b = SOC_{x,t-1}^b + \frac{(\eta^{b+}.P_{x,t}^{b+} - \frac{P_{x,t}^{b-}}{\eta^{b-}}) \cdot \Delta t}{E_x^b} \tag{3}$$

where $SOC_{x,t}^b$ represents the battery state of charge in microgrid x during time t, $P_{x,t}^{b+}$ and $P_{x,t}^{b-}$ refer to the battery charging/discharging powers, with charging/discharging efficiencies η^{b+} and η^{b-}, during the time step Δt. E_x^b denotes the battery nominal capacity.

2.4 Network model

To achieve global optimality, the MMG network model is embedded within the EMS. The AC power flow is described as follows [5]:

$$P_{x,t} = \sum_{\substack{y=1 \\ y \neq x}}^{N} |v_{x,t}||v_{y,t}|(g_{xy}.\cos(\theta_{x,t} - \theta_{y,t}) + b_{xy}.\sin(\theta_{x,t} - \theta_{y,t})) \tag{4}$$

$$Q_{x,t} = \sum_{\substack{y=1 \\ y \neq x}}^{N} |v_{x,t}||v_{y,t}|(g_{xy}.\sin(\theta_{x,t} - \theta_{y,t}) - b_{xy}.\cos(\theta_{x,t} - \theta_{y,t})) \tag{5}$$

where $P_{x,t}$ and $Q_{x,t}$ represent the active and reactive power injections at bus x at time t, v_x and v_y represent the voltage magnitudes at buses x and y, while θ_x and θ_y correspond to the associated voltage phase angles, g_{xy} and b_{xy} correspond to the conductance and susceptance of the transmission line connecting buses x and y, and N is the total number of buses in the network.

3 Optimization and Planning of the MMG

The optimization model is formulated to optimize the performance of the MMG through effective management of energy exchanges between microgrids, local generation, storage units, and the utility grid.

3.1 Objective function

The objective function aims to minimize the total MMG operational cost (OC), which includes costs associated with PV, WT, the battery, and grid energy transactions:

$$\min \sum_{t} \left(\sum_{x} \left(OC^{b}_{x,t} + OC^{pv}_{x,t} + OC^{wt}_{x,t} \right) + C_{grid,t} \right) \tag{6}$$

$$OC^{pv}_{x,t} = P_{pv_{x,t}} \frac{C^{pv}_{\text{inv}} + \sum_{i=1}^{n} C^{pv}_{\text{om}}(1+dr)^{-i}}{\sum_{i=1}^{n} E^{pv}_{\text{an}}(1-\sigma^{pv})^{i-1}(1+dr)^{-i}} \tag{7}$$

$$OC^{wt}_{x,t} = P_{wt_{x,t}} \frac{C^{wt}_{\text{inv}} + \sum_{i=1}^{n} C^{wt}_{\text{om}}(1+dr)^{-i}}{\sum_{i=1}^{n} E^{wt}_{\text{an}}(1-\sigma^{wt})^{i-1}(1+dr)^{-i}} \tag{8}$$

$$OC^{b}_{x,t} = (\eta^{b+} P^{b+}_{x,t} + \frac{P^{b-}_{x,t}}{\eta^{b-}}).\frac{1}{2} \frac{\left(C^{b}_{\text{inv}} + \sum_{i=1}^{n} C^{b}_{\text{om}}(1+dr)^{-i} \right)(1+dr)^{n} - RV}{(1+dr)^{n} \chi^{E}_{T} \chi^{\Upsilon}_{T} \chi^{\Upsilon}_{d} \Upsilon^{b}_{r} E^{b}_{r}} \tag{9}$$

$$C_{\text{grid},t} = \pi^{+}_{g_t} P^{+}_{g_t} - \pi^{-}_{g_t} P^{-}_{g_t} \tag{10}$$

where, $P_{pv_{x,t}}$, $P_{wt_{x,t}}$, $P^{+}_{g_t}$ and $P^{-}_{g_t}$ are the scheduled PV, WT power, the power taken from the grid and the power sold to the grid, respectively. The OC considers the degradation of the equipments and incorporates the investment cost (C_{inv}), operation and maintenance costs (C_{om}), annual energy generation (E_{an}), discount rate (dr), and the degradation rate (σ) over the system lifetime n [6]. A battery degradation cost model (BDC) for a lithium-ion battery is taken from [7] and includes the normalized temperature-dependent capacity fading (χ^{E}_{T}), the temperature and DOD dependent cycle life fading coefficients ($\chi^{\Upsilon}_{T}, \chi^{\Upsilon}_{d}$). E^{b}_{r} and Υ^{b}_{r} are the rated energy capacity and the battery life cycle. RV is the battery residual value remaining at the end of its lifespan.

3.2 Power balance Constraint

The EMS is designed to optimize the distribution of power throughout the MMG network by reducing energy losses and ensuring balance between generation, storage, and demand at each time step t:

$$\sum_{x} \left(P_{pv_{x,t}} + P_{wt_{x,t}} + P^{b-}_{x,t} - P^{b+}_{x,t} \right) + P_{g_t} = \sum_{x} D^{p}_{x,t} \tag{11}$$

3.3 Network stability constraint

The voltage magnitudes $v_{x,t}$ and phase angles $\theta_{x,t}$ at each bus x are restricted within acceptable bounds to guarantee system stability and secure operation:

$$v^{\min}_{x} \le v_{x,t} \le v^{\max}_{x} \tag{12}$$

$$\theta^{\min}_{x} \le \theta_{x,t} \le \theta^{\max}_{x} \tag{13}$$

3.4 Grid Interaction

The energy transferred to or from the main grid is constrained to meet contractual agreements and technical requirements:

$$P_g^{\min} \leq P_{g_t} \leq P_g^{\max} \tag{14}$$

3.5 Battery constraints

To preserve battery health and extend its service life, the battery operation is constrained such that charging and discharging cannot occur simultaneously (15), while the charging/discharging power (16) (17), SOC, and depth of discharge (DOD) limits (18) must be satisfied. Furthermore, a cyclic constraint is imposed such that the battery SOC at the end of the scheduling horizon equals its initial value, thereby ensuring energy availability for the subsequent operating day (19):

$$P_{x,t}^{b+} \cdot P_{x,t}^{b-} = 0 \tag{15}$$

$$0 \leq P_{x,t}^{b-} \leq P_{\max,x}^{b-} \tag{16}$$

$$0 \leq P_{x,t}^{b+} \leq P_{\max,x}^{b+} \tag{17}$$

$$(SOC_x^{\max} - DOD_x) \leq SOC_{x,t}^{b} \leq SOC_x^{\max} \tag{18}$$

$$SOC_{x,t_s}^{b} = SOC_{x,t_f}^{b} \tag{19}$$

3.6 Reactive Power Coordination

In the MMG system, reactive power management is crucial to maintain voltage stability and ensure the secure operation of the network. Each resource, including photovoltaic (PV) units, wind turbines (WT), batteries, and the grid connection, must operate within their apparent power limits to coordinate the exchange of both active and reactive power. The following constraints guarantee that the apparent power of each device does not exceed its rated capacity:

$$P_{g_t}^2 + Q_{g_t}^2 \leq S_g^2 \tag{20}$$

$$P_{pv_{x,t}}^2 + Q_{pv_{x,t}}^2 \leq S_{pv_x}^2 \tag{21}$$

$$P_{wt_{x,t}}^2 + Q_{wt_{x,t}}^2 \leq S_{wt_x}^2 \tag{22}$$

$$(P_{x,t}^{b+} - P_{x,t}^{b-})^2 + (Q_{x,t}^{b})^2 \leq (S_x^{b})^2 \tag{23}$$

4 Results and discussion

The model is developed using the authors' customized MATLAB code based on a nonlinear mixed programming (NLP) approach. Simulations were carried on a computer equipped with an Intel i7 processor (1.90 GHz) and a 16 GB RAM. The optimization is performed over a 24-hour simulation horizon with a one-hour time step.

4.1 Input Data

Economic data are taken from [8], technical characteristics of the components are detailed in Table 1. The time-of-use (TOU) electricity prices (in €/kWh) utilized in the simulations are presented in Fig. 2 [9].

The city of Casablanca, Morocco, is chosen as a case study. Meteorological data are used for a typical sunny day (Fig. 3). According to historical data from [10], Casablanca has an average yearly global horizontal irradiation of approximately 5.2 kWh/m²/day and an average wind speed of around 5.0 m/s. The power demands are shown in Fig. 4.

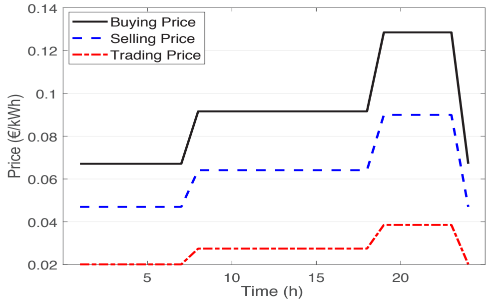

Figure 2. TOU energy prices.

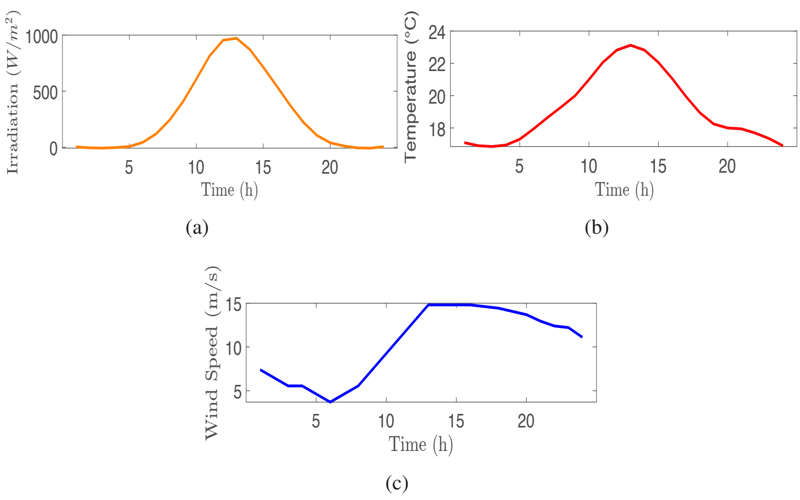

Figure 3. Weather data. (a) Solar irradiation. (b) Temperature. (c) Wind speed.

Table 1. Technical data.

	P_{pv}^{ins} (kWc)	S_{pv} (kVA)	P_{wt}^{ins} (kWc)	S_{wt} (kVA)	E^b (kWh)	S^b (kVA)
MG1	4.3	4.6	2.2	2.3	39.9	1.8
MG2	7	7.3	5.5	5.7	80	3.6
MG3	11.2	11.8	9.4	9.9	129.9	6
MG4	8.1	8.5	3.1	3.3	59.9	3.2

4.2 Simulations results

The numerical results provide important insights into the operational behavior and techno-economic feasibility of the proposed MMG system.

Fig. 5 shows the energy management across interconnected MGs and the main grid. Results demonstrate that the EMS effectively coordinates local production, storage, and exchanges with the main grid. This coordination manages consumption peaks and makes optimal use of favorable periods, by taking into account TOU tariffs (Fig. 2). The adopted strategy minimizes operational costs by reducing reliance on the main grid when renew-

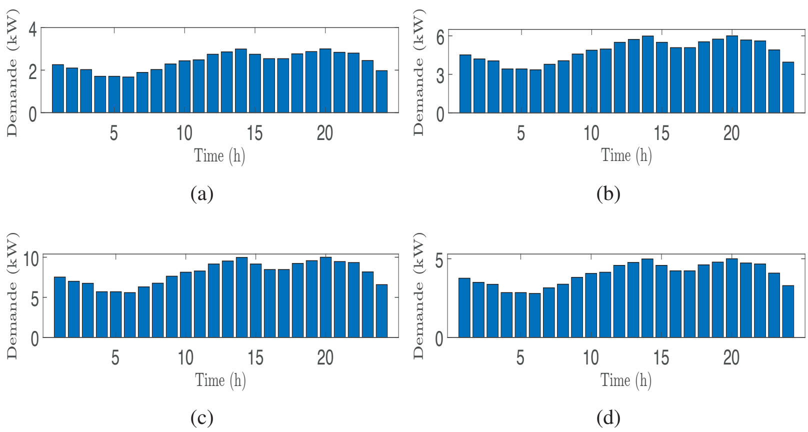

Figure 4. Power demands. (a) MG1. (b) MG2. (c) MG3. (d) MG4.

able ressources and storage are sufficient to cover demand. Moreover, the energy flows between microgrids help balance local discrepancies by redistributing excess energy from one microgrid to another with higher demand. This mechanism contributes to improved self-consumption and overall reduced dependence on the main grid.

The operating cost distribution per day, as illustrated in Fig. 6, provides insights into the cost structure of each MG and the overall MMG system. The total daily cost for the MMG is 15.40 €, with individual MGs contributing differently based on their energy consumption and resource utilization. Each MG exhibits a unique cost composition depending on its energy mix. MG2 and MG3 rely more on battery storage (47 % and 52 %), which indicate higher self-consumption strategies. MG1 and MG4, in contrast, have a more proportion of transactions (55 % and 54 %), suggesting a stronger dependence on energy exchanges within the MMG and the main grid. At the MMG level, PV and WT account for 10.9 % and 14.02 % of the total cost, respectively, while battery costs represent 35.5 %, primarily due to degradation and replacement costs. Transactions with the main grid contribute the largest share at 39.7 % of the total cost. For MGs connected to the grid, energy trading with neighboring MGs successfully compensates 12.3 % of transaction costs, which explains the preference for selling energy to neighboring MGs to support deficit areas rather than injecting it into the grid. Additionally, the cost distribution remains balanced across MGs, regardless of variations in demand. This is due to the effective integration of energy trading, allowing MGs to compensate for deficits through intra-MMG exchanges rather than relying solely on the main grid. As a result, MGs can mitigate high grid dependency and optimize cost efficiency through coordinated energy management.

5 Conclusion

This article highlighted the role of MMG systems in enhancing energy management and reducing operational costs through the coordinated integration of renewable energy solutions, storage systems, and advanced energy management strategies. By incorporating dynamic energy management, MMGs provide improved resilience and flexibility for power networks. Future work will focus on expanding the optimization framework by incorporating multi-objective techniques and advanced algorithms to enhance the computational efficiency of both sizing and energy management, integrating more aspects such as Demand Response

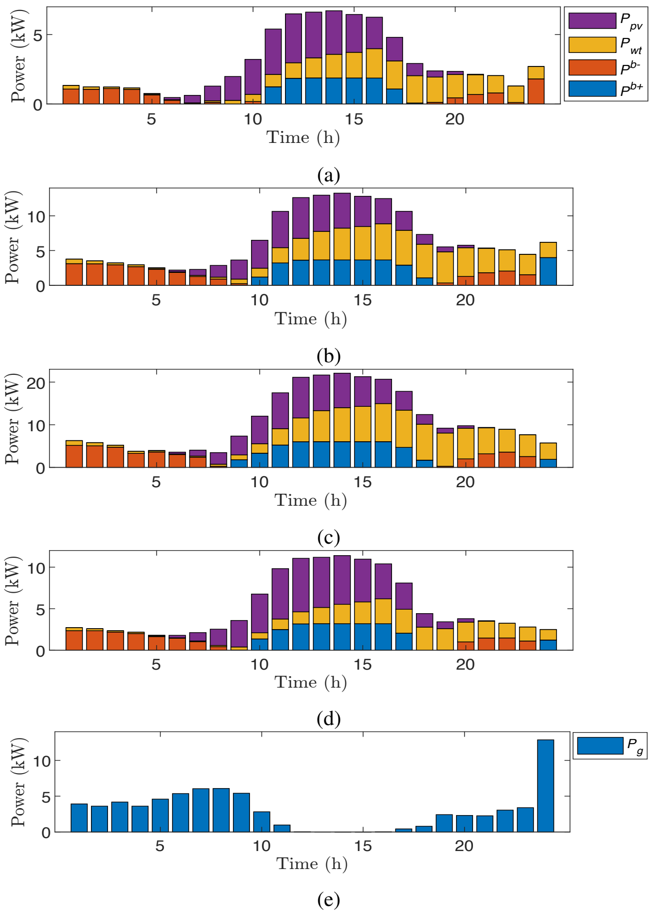

Figure 5. Energy management results. (a) MG1. (b) MG2. (c) MG3. (d) MG4. (e) Main grid.

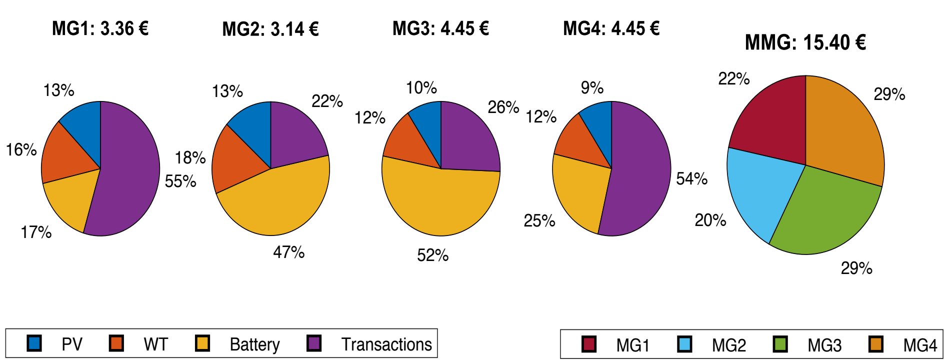

Figure 6. Operating costs per day with DER generations percentage and MGs contribution percentage.

(DR) strategies for improved system flexibility and performance. Additionally, further studies should explore the impact of seasonal variability and islanding operation cases to to enhance the resilience of MMG systems.

Acknowledgement : The authors acknowledge the financial support from ISEN Yncréa Ouest, Nantes and PHC Toubkal under grant number N° : TBK/24/185 N°CAMPUS : 49960SJ. With the support of the CNRST as part of the "PhD-ASsociate Scholarship – PASS" Program.

References

1. A. Akter, E.I. Zafir, N.H. Dana, R. Joysoyal, S.K. Sarker, L. Li, S.M. Muyeen, S.K. Das, I. Kamwa, A review on microgrid optimization with meta-heuristic techniques: Scopes, trends and recommendation, Energy Strat Rev **51**, 101298 (2024). https://doi.org/10.1016/j.esr.2024.101298
2. S. Ahmad, M. Shafiullah, C.B. Ahmed, M. Alowaifeer, A review of microgrid energy management and control strategies, IEEE Access **11**, 21729 (2023). 10.1109/ACCESS.2023.3248511
3. O.M. Babatunde, J.L. Munda, Y. Hamam, A comprehensive state-of-the-art survey on hybrid renewable energy system operations and planning, IEEE Access **8**, 75313 (2020). 10.1109/ACCESS.2020.2988397
4. G.N.N. Dessalegn Bitew Aeggegn, C. Wekesa, A state of the art review on energy management techniques and optimal sizing of ders in grid-connected multi-microgrids, Cogent Eng **11**, 2340306 (2024), `https://doi.org/10.1080/23311916.2024.2340306`. 10.1080/23311916.2024.2340306
5. Hale Cetinay, Saleh Soltan, Fernando A. Kuipers, Gil Zussman and Piet Van Mieghem , Comparing the Effects of Failures in Power Grids Under the AC and DC Power Flow Models, IEEE Trans Netw Sci Eng **5**, 301 (2018). 10.1109/TNSE.2017.2763746
6. M.F. Zia, E. Elbouchikhi, M. Benbouzid, J. Guerrero, Energy management system for an islanded microgrid with convex relaxation, IEEE Trans Ind Appl **55**, 7175 (2019). 10.1109/TIA.2019.2917357
7. M.F. Zia, E. Elbouchikhi, M. Benbouzid, Optimal operational planning of scalable dc microgrid with demand response, islanding, and battery degradation cost considerations, Appl Energy **237**, 695 (2019). https://doi.org/10.1016/j.apenergy.2019.01.040
8. S. Singh, M. Singh, S.C. Kaushik, Feasibility study of an islanded microgrid in rural area consisting of pv, wind, biomass and battery energy storage system, Energy Convers Manag **128**, 178 (2016). https://doi.org/10.1016/j.enconman.2016.09.046
9. Office National de l'Électricité et de l'Eau Potable (ONEE) - Maroc, Tarif général de l'électricité, https://www.one.org.ma/FR/pages/, last accessed 14/03/2025
10. NASA Langley Research Center, NASA prediction of worldwide energy resources (POWER) data access viewer, https://power.larc.nasa.gov/data-access-viewer/, last accessed 2025-03-05